Recombinant Microtubule-Associated Protein 2c Reduces the Dynamic Instability of Individual Microtubules†

T. Chris Gamblin,‡ Kirsten Nachmanoff,§ Shelley Halpain,§ and Robley C. Williams, Jr.*,‡

Department of Neuroscience and Center for Cell Signalling, University of Virginia, Charlottesville, Virginia 22908, and Department of Molecular Biology, Vanderbilt University, Nashville, Tennessee 37235

Received May 14, 1996; Revised Manuscript Received July 22, 1996⊗

ABSTRACT: The effects of purified recombinant microtubule-associated protein 2c (rMAP2c) on the dynamic instability of microtubules were examined by direct observation of individual microtubules *in vitro* by video-enhanced differential interference contrast light microscopy. Microtubules were grown in the absence or presence of varying concentrations of rMAP2c and were analyzed to determine growth rates, shortening rates, and the frequencies of conversion between growing and shortening phases. We found rMAP2c to stabilize microtubules dramatically. The most notable effect is a reduction in both the frequency of catastrophes (transitions from growth to shortening) and the mean length of shortening events: no microtubule catastrophes were observed at concentrations of rMAP2c as low as 1.06 μM in a solution of 10 μM tubulin. Even at lower rMAP2c concentrations, there is a marked stabilizing effect. As the concentration of rMAP2c increases, average growth rates increase slightly, shortening rates decrease, and the frequency of rescues (transitions from shortening to growth) increases significantly. Together, these changes in parameters produce a population of extremely stable microtubules in the presence of rMAP2c. This stabilization is consistent with a structural role for MAP2c during early postnatal neural development.

Microtubules are important biological macromolecular complexes with a wide variety of functions. They form the interphase array in animal cells, helping to maintain the cytoskeleton during cell growth. They also form the mitotic spindle in dividing cells, separating the daughter chromosomes to give rise to new cells. They contribute to the cytoskeleton of differentiated cells, such as the polarized parallel array of epithelial cells and the staggered linear array in axons and dendrites of neurons (Cassimeris, 1993).

Microtubules exhibit dynamic instability (Mitchison & Kirschner, 1984a,b) both *in vitro* (Mitchison & Kirschner, 1984a,b; Horio & Hotani, 1986; Walker et al., 1988; Gildersleeve et al., 1992) and *in vivo* (Sammak & Borisy, 1988; Schulze & Kirschner, 1988; Cassimeris et al., 1988; Okabe & Hirokawa 1988; Shelden & Wadsworth, 1993; Hush et al., 1994), visible as large excursions of growth and shortening. These are thought to be caused by the presence of a hypothetical "GTP cap". Tubulin dimers bearing bound GTP at their exchangeable nucleotide-binding site are added to the ends of microtubules, resulting in growth of the structure. As this polymerization proceeds and subunits become "buried" beneath newly added ones, their GTP is hydrolyzed to GDP, leaving a "cap" of newly added tubulin dimers that still contain GTP. The GTP cap stabilizes a microtubule against depolymerizaion, but is itself evanescent. Its random loss is thought to lead to rapid disassembly of the microtubule (termed a "catastrophe"); its reacquistion is thought to lead to regrowth (termed "rescue"). Dynamic instability allows the array of microtubules to be periodically remodeled. Subunits released by depolymerization in one part of a cell can repolymerize elsewhere to perform new functions.

How dynamic instability is regulated, or modulated, to allow microtubules to perform different cellular functions has long been a mystery. It is clear that binding of microtubule-associated proteins (MAPs[1]) may produce some modulation (Murphy & Borisy, 1975; Murphy et al., 1977; Cleveland et al., 1977; Mitchison & Kirschner, 1984b; Sloboda et al., 1976; Job et al., 1985; Bré & Karsenti, 1990; Pryer et al., 1992; Drechsel et al., 1992; Yamauchi et al., 1993; Kowalski & Williams, 1993; Vasquez et al., 1994; Ainsztein & Purich, 1994; Olesen, 1994; Panda et al., 1995). MAP2, for instance, has been shown to promote overall microtubule growth *in vitro* in all of the four possible ways: increasing the rate of growth and the frequency of rescue while decreasing the rate of shortening and frequency of catastrophe (Kowalski & Williams, 1993). Similar results have been obtained for the microtubule-associated protein tau for growing microtubules (Drechsel et al., 1992). The addition of tau to steady-state microtubules suppresses dynamic instability by reducing the mean rate of shortening and growing, strongly increasing the rate of rescue, and slightly decreasing the rate of catastrophe (Panda et al., 1995). *In vivo*, the picture may be more complex. Microinjection of purified MAPs into BSC-1 cells led to a reduction in microtubule dynamic instability by decreasing

† Supported by Grants GM 25638 (R.C.W.) and MH 50861 (S.H.) of the National Institutes of Health and by the Vanderbilt University Research Council and the University of Virginia Center for Cell Signalling.

* Author to whom correspondence should be addressed. Telephone: 615-322-2072. Fax: 615-343-6707. E-mail: williarc@ctrvax.vanderbilt.edu.

‡ Vanderbilt University.

§ University of Virginia.

⊗ Abstract published in *Advance ACS Abstracts,* September 1, 1996.

[1] Abbreviations: DIC, differential interference contrast; MAP, microtubule-associated protein; PBS, phosphate-buffered saline (120 mM NaCl, 2.7 mM KCl, and 10 mM phosphate buffer, pH 7.4, at 25 °C); PMD buffer, 0.1 M Pipes, pH 6.9, 1 mM $MgSO_4$, 2 mM EGTA, 2 mM dithioerythritol, 1 mM GTP; rMAP2c, recombinant microtubule-associated protein 2c.

S0006-2960(96)01135-X CCC: $12.00

the magnitude of dynamic events and increasing the time the microtubules spent in an attenuated phase, when they neither grew nor shortened (Dhamodharan & Wadsworth, 1995). Due to the difficulty in measuring microtubule dynamics *in vivo*, though, these experiments had a length resolution of ~0.5 μm, and a reduced time resolution of only 1 image every 2 s, making the measurement of rates below 1 μm/min a practical impossibility. Transient or stable overexpression of many MAPs in nonneuronal cell lines leads to massive polymerization and bundling of microtubules, similar to the microtubule organization seen in neurite extensions (Lewis et al., 1989; Kanai et al., 1989; Baas et al., 1991; Knops et al., 1991; Chen et al., 1992; Gallo et al., 1992; Takemura et al., 1992, 1995; Weisshaar et al., 1992; Umeyama et al., 1993; LeClerc et al., 1993, 1996; Weisshaar & Matus, 1993; Knowles et al., 1994). Results thus far, with the exception of those obtained with recombinant tau protein, have come from experiments in which the details of the molecular state of the added MAPs could not be fully ascertained. MAPs isolated from tissue are inevitably a mixture of molecules bearing a variety of posttranslational modifications. Polypeptides expressed or microinjected into cells may also undergo modification before their incorporation into microtubules. MAPs expressed *in vivo* have been shown to undergo differential posttranslational modifications during neuronal development, changes which could play an important role in MAP function (Riederer, 1992; Sanchez et al., 1995). As a step toward clarifying the role that posttranslational modification of MAPs may play, it would be advantageous to utilize a homogeneous molecule whose state of posttranslational modification could be specified fully. Insight into MAP2's interactions with microtubules has come from studies using bacterially expressed constructs encoding the carboxyl-terminal microtubule binding regions (Coffey & Purich, 1995). However, it is important to recognize that the domains ouside the microtubule binding region could potentially influence the interaction of MAP2 with microtubules, as is the case with the related protein MAP4 (Olson et al., 1995).

Microtubule-associated protein 2c (MAP2c) is a developmentally regulated splicing product of the gene encoding MAP2, a neuron-specific MAP, which also encodes the high molecular weight splice variants MAP2a and MAP2b (Garner & Matus, 1988; Chung et al., 1996). MAP2c consists of the amino-terminal and carboxyl-terminal ends of MAP2b, lacking approximately the middle two-thirds of the sequence. All three isoforms of MAP2 contain a nonidentical 18 amino acid triad within the carboxyl-terminal microtubule binding region. In the rat brain, MAP2c begins to appear a few days before birth along with MAP2b. MAP2c is abundantly expressed in dendrites through the first 10 postnatal days, during which time extensive dendritic growth and arborization take place. From day 10 to day 20, MAP2c levels decrease substantially until they are approximately 5% of early postnatal expression (Riederer & Matus, 1985; Charriere-Bertrand et al., 1991). During this period in which MAP2c levels drop, dendritic growth slows and synaptogenesis peaks. A few CNS regions that undergo neuritigenesis throughout postnatal life, such as the olfactory bulb and the retina, continue to express MAP2c at high levels into adulthood (Tucker, 1990). These observations have led to the suggestion that MAP2c participates in neurite outgrowth, but that it is not principally involved in later stages of neuronal maturation, when morphological changes are less extensive.

To assess the role that MAP2c could play in the process of neuronal outgrowth, it is necessary to understand the effects that it has on the dynamic instability of individual microtubules. In this paper we report the characterization, by video-enhanced DIC light microscopy, of the dynamic instability of individual microtubules assembled from mixtures of tubulin and recombinantly produced MAP2c. Rates of growth and shortening and frequencies of transition between growth and shortening (catastrophe and rescue), when averaged over a population of microtubules, describe the extent of dynamic instability for that population. Variation of these quantities with concentration of rMAP2c reveals the details of its effects on dynamic instability. At relatively high concentrations of rMAP2c, catastrophes were completely suppressed, resulting in microtubules that exhibited only growth. The growth rates of these microtubules were also increased slightly. At lower concentrations of rMAP2c, the growth rates and frequency of catastrophe were largely unaffected, but the frequency of rescue was increased, the shortening rates were decreased, and the average length of a shortening event was decreased. These effects, taken together, indicate that MAP2c promotes the formation of long stable arrays of microtubules.

MATERIALS AND METHODS

Reagents. Pipes buffer was from Boehringer Mannheim (Indianapolis, IN), carrier-free $Na^{125}I$ was from ICN (Costa Mesa, CA), and taxol was purchased from Calbiochem as a dry powder and was dissolved in DMSO to make a 10 mM stock solution. Restriction enzymes were purchased from Promega Corp. (Madison, WI). Phosphate buffered saline (PBS), used as the reaction buffer for iodination experiments, was purchased as a dry powder from Sigma (St. Louis, MO). All microtubule assembly and MAP2c-binding experiments were carried out in PMD buffer (0.1 M Pipes, pH 6.9, 1 mM $MgSO_4$, 2 mM EGTA, 2 mM dithioerythritol, and 1 mM GTP).

Tubulin, MAP2c, and Chlamydomonas Flagellar Axonemal Pieces. Microtubule protein was prepared from bovine brain by 3 cycles of temperature-dependent assembly/disassembly (Williams & Lee, 1982). Tubulin was purified from microtubule protein by chromatography on either phosphocellulose (Williams & Lee, 1982; Correia et al., 1987) or DEAE-Sephadex (Vallee, 1986). No differences in results were noted between the two preparations. Phosphocellulose-purified tubulin was used in microscope experiments (Figure 1); microtubules assembled from DEAE-tubulin were used as the substrate for MAP2c binding experiments.

A cDNA encoding full length rat MAP2c was assembled by ligating the 5′ *Nde*1−*Pst*1 restriction enzyme fragment of clone pCG2b33 (Kindler et al., 1990) to the 3′ *Pst*1−*Bam*H1 restriction enzyme fragment of clone pJBMap2C (Berling et al., 1994) and unidirectionally subcloning it into the *Nde*1 and *Bam*H1 sites of the pET3a expression vector (Novagen, Madison, WI). Plasmids pCG2b33 and pJBMap2c were both gifts of Dr. Craig Garner, University of Alabama, Birmingham. The nucleotide sequence was verified by DNA

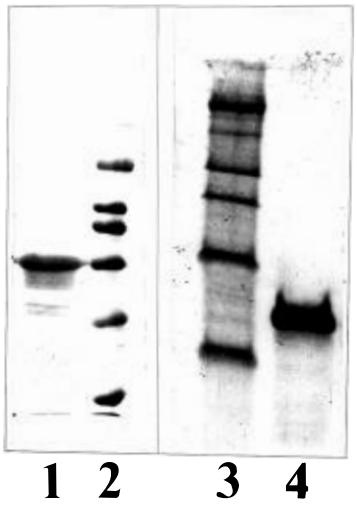

FIGURE 1: SDS−PAGE analysis of purified tubulin and rMAP2c. Tubulin and rMAP2c were purified as described in Materials and Methods. Lane 1: purified rMAP2c. Lane 2: Molecular weight standands. Lane 3: Molecular weight standards. Lane 4: purified 3X-PC tubulin used in microscopic studies.

sequencing by means of the Sequenase Kit version 2.0 from United States Biochemical, Inc. (Cleveland, OH). We designated the plasmid construct containing the pET3a vector and full length rat MAP2c cDNA as pET3aMAP2c. pET3aMap2c was transformed into competent *Escherichia coli* strain BL21(DE3) (Novagen) and grown in Luria broth + ampicillin (100 μg/mL) to an $A_{600} = 0.6-0.8$. To induce protein expression, isopropyl β-thiogalactopyranoside was added to 0.4 mM, and the cells were grown for an additional 3 h and then harvested by centrifugation at 5000*g*. Bacterial pellets from 25−50 mL of culture were resuspended in 1 mL of 50 mM Tris-HCl, pH 8.0, containing 2 mM EDTA, 0.1% Triton X-100, and 0.1 mg/mL lysozyme, and the solution was incubated for 15 min at 30 °C. Protease inhibitors were added to the following final concentrations: 1 mM PMSF, 10 mg/mL aprotinin, 2.5 mg/mL pepstatin, 5 mg/mL leupeptin. Samples were sonicated for several seconds on ice to lyse the cells and break up DNA. The lysate was centrifuged for 25 min at 39000*g* to spin out insoluble material. The supernatants were transferred to fresh tubes and brought to pH 7.5 by addition of 1 N HCl. NaCl was added to a final concentration of 0.75 M and β-mercaptoethanol was added to 2%. The solution was placed in a boiling water bath for 8 min, cooled on ice for 10 min, and then centrifuged for 25 min at 10000*g*. The supernatant, which contains the heat-stable proteins, chiefly rMAP2c, was removed and buffer exchanged into 50 mM HEPES, pH 7.4, 1 mM $MgCl_2$, 1 mM EGTA, 1 mM EDTA, 2 mM dithiothreitol, and 2 mM β-mercaptoethanol by means of a PD-10 column (Pharmacia, Piscataway, NJ). Column fractions were collected and analyzed for protein content. Fractions containing purified rMAP2c were pooled and frozen in liquid nitrogen and stored at −80 °C. MAP2c was estimated to be 98% pure as determined by SDS−PAGE on 8% gels stained with Coomassie blue (Figure 1). The minor, higher mobility bands detected by this method were all recognized by MAP2-specific antibodies in immunoblot analyses (not shown), indicating they result either from proteolytic breakdown of rMAP2c or incomplete transcription/translation of the cDNA.

Chlamydomonas flagellar axonemal pieces were isolated by the dibucaine-HCl method (Witman, 1986) from *Chlamydomonas reinhardtii* strain CC-125 and prepared for use as described by Gamblin and Williams (1995). Their use as nucleating structures for microtubule growth allows one to determine the polarity of single microtubules from the distinctive appearance of the two axonemal ends (Gamblin & Williams, 1995).

^{125}I Iodination of rMAP2c. rMAP2c was exchanged into PBS, pH 7.4, by means of a Bio-Rad Biospin-5 column (Hercules, CA). Pierce Iodo-beads (Pierce Chemical Co., no. 28665, Great Falls, VA) were prepared for use by washing with PBS and drying on filter paper. Five beads were preincubated with 5 mCi of $Na^{125}I$ for 5 min at room temperature. rMAP2c (500 μg in various volumes of PBS, pH 7.4, depending on the concentration of rMAP2c) was added to the Iodo-beads and incubated for 15 min at room temperature. The reaction was stopped by removing the protein from the reaction solution by pipette (Markwell, 1982). The rMAP2c was exchanged into PMD buffer, and the protein concentration was determined by the method of Bradford (1976). The specific activity of the protein was determined by measuring the radioactivity contained in a sample of protein of known concentration. The amount of free ^{125}I remaining in solution was determined by centrifuging a sample through a Millipore (Marlborough, MA) 30 000 MW cutoff filter (type PLTK filter). Approximately 10% of the total radioactivity in the protein sample appeared in the filtrate and was deemed to be free ^{125}I.

rMAP2c Binding Isotherm. A centrifugation assay similar to the one described by Vallee (1982) was used to assess the binding of rMAP2c to taxol-stabilized microtubules. Stabilized microtubules were prepared by incubating 124 μM tubulin in PMD buffer + 0.2% NaN_3 with an equimolar amount of taxol. The solution was then passed several times through a 26-gauge × 3/8 in. needle to shear the resulting microtubules. ^{125}I-labeled rMAP2c in PMD was then added to microtubule solutions to achieve a final microtubule concentration of 1 μM, and the mixture was incubated in cellulose propionate centrifuge tubes at 37 °C for 45 min to allow rMAP2c to bind to the microtubules. To prevent nonspecific adsorption of rMAP2c to the plastic tubes, they were precoated by incubation with bovine serum albumin (10 mg/mL) at room temperature for 10 min. Less than 4% of the rMAP2c adsorbed to these coated tubes following this procedure. The reaction mixtures were centrifuged in a Beckman Airfuge at 30 psi (∼149000*g* in the A-100/18 rotor) for 10 min at room temperature. Supernatant and pellet were separated and analyzed for ^{125}I-labeled rMAP2c content by scintillation counting in a Beckman LS 700 instrument. To determine whether aggregates of iodinated rMAP2c pelleted in a microtubule-independent fashion at very high rMAP2c concentrations, a microtubule-free control was performed.

Light Microscopy. Microtubules were visualized by video-enhanced differential-interference contrast light microscopy with a Zeiss Axiovert 35 microscope maintained at 34 °C. Images were processed by a Hamamatsu Argus-10 and recorded on a Mitsubishi Super-VHS VCR (Schnapp, 1986; Williams, 1992). Samples were prepared by introducing *Chlamydomonas* flagellar axonemal pieces into a chamber constructed between a coverslip and slide with parafilm spacers (Williams, 1992). The chamber was inverted and incubated at room temperature for a short period to allow

the axonemal pieces to settle and adhere to the coverslip. To saturate the internal surfaces of the chamber with adsorbed proteins, three chamber volumes of the reaction mixture, consisting of 10 μM tubulin and the particular concentration of rMAP2c, were caused to flow through the reaction chamber. A fourth chamber volume of the reaction mixture was then introduced as the actual experimental sample. The reaction chamber was sealed with Valap, a 1:1:1 mixture of Vaseline, lanolin, and paraffin. Specimens were kept on ice prior to observation and were warmed by contact with the microscope stage. They were discarded after 1 h at 34 °C.

Electron Microscopy. Microtubules were grown on copper grids coated with Formvar and carbon and examined in a Philips CM12 transmission electron microscope. A 5-μL drop containing *Chlamydomonas* flagellar axonemal pieces was first placed on a freshly glowed grid for 60 s, and then the excess liquid was removed by blotting. A mixture of 15 μM tubulin and 3.7 μM rMAP2c in PMD buffer was applied to the grid and incubated at 37 °C for 5 min. The grid was then rinsed with seven drops of 0.1 M ammonium acetate, pH 6.9, + 1 mM GTP and stained with 1% uranyl acetate for 30 s.

Data Analysis. Microtubules were measured and analyzed by the use of a computer program similar to those described by Gildersleeve et al. (1992) and by Kowalski and Williams (1993). Measurements of the length of a microtubule were recorded at intervals of approximately 5 s. In addition, all shortening events at all concentrations of rMAP2c were measured in slow motion playback at one-eighth speed. This was done to improve accuracy in measurements, because shortening occurs at a much more rapid speed than growth. The length−time profiles thus obtained were then automatically scanned by a second program to obtain rates of growth and shortening and to identify catastrophes and rescues. The rate of growth or shortening corresponding to a particular time point was measured by selecting a number of adjacent points, usually five on each side, fitting a quadratic equation to the local curve of length vs time which they describe, and obtaining the slope at the middle point (i.e., the rate of growth or shortening) as well as the standard deviation of the slope (i.e., its statistical uncertainty). The next point was then selected as the middle point for fitting and the process repeated, until all time points of a particular microtubule had been treated. These successive measurements of slopes and their uncertainties were used to find the occurrences of catastrophes and rescues in a statistically well-defined way, as follows. First, each slope was categorized as being certainly positive, certainly negative, or indeterminate, according to whether its absolute value differed from zero by more than 1.65 times its standard deviation (95% confidence). Then this list of categories was used to identify transitions between growth and shortening. A catastrophe was deemed to occur when a period of growth (i.e., one or more windows of certainly positive slope) was followed by a period of shortening (one or more windows of certainly negative slope) or by one or more windows of indeterminate slope followed by shortening. A rescue was similarly detected, although with opposite signs of the successive slopes. When the same data set was examined by this algorithm and by those previously used (Gildersleeve et al., 1992; Kowalski & Williams, 1993), the frequencies of transitions and the distributions of growth and shortening rates were found to agree well. The current algorithm, though, provides a statistically objective measure of the quantities involved.

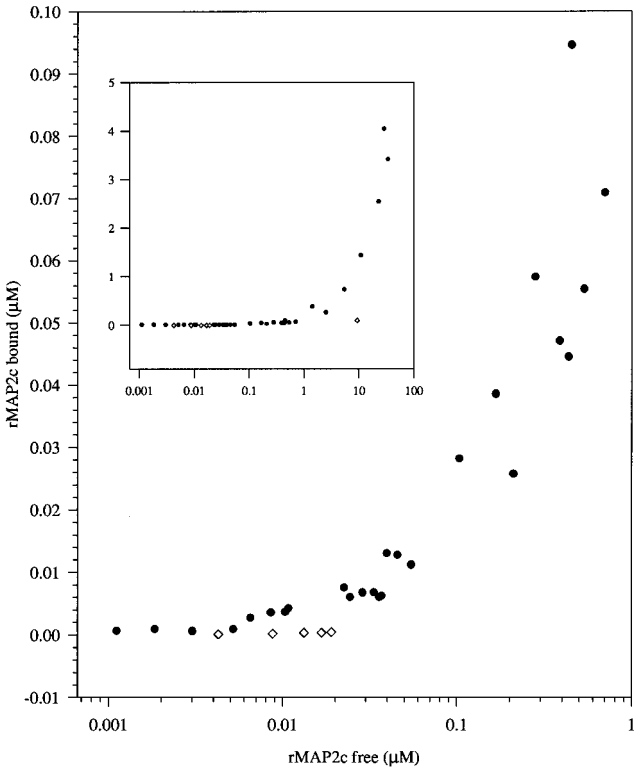

FIGURE 2: Binding isotherm (expanded scale) for rMAP2c binding to taxol-stabilized microtubules. rMAP2c was labelled with ^{125}I to facilitate detection. Microtubule-bound rMAP2c was separated from free rMAP2c in solution by ultracentrifugation (see Materials and Methods) (solid circles). The horizontal axis shows the concentration of free MAP2c, calculated from the specific activity of radioactively iodinated rMAP2c, on a logarithmic scale. The vertical axis shows the concentration of rMAP2c bound to taxol-stabilized microtubules. The inset shows entire binding isotherm. The amounts of rMAP2c that pelleted in the absence of microtubules in this assay are represented by open diamonds.

RESULTS

The sedimentation assay yielded the isotherm shown in Figure 2 for the binding of rMAP2c to microtubules. Its most striking aspect is the apparent lack of saturation of the binding even at a concentration of 37.4 μM rMAP2c, a ~40-fold molar excess over tubulin dimer (inset, Figure 2). At this point on the binding curve, approximately 4 mol of rMAP2c are bound for every mole of tubulin dimer present in microtubules. Control experiments in which microtubules were omitted from the assay yielded only background amounts of pelleted rMAP2c, indicating that the large extent of apparent binding is not caused by microtubule-independent aggregation and pelleting of the protein (open diamonds, Figure 2, and inset, Figure 2). Given the molecular dimensions of tubulin and MAP2c, it appears that molecules of rMAP2c must associate not only with the tubulin molecules of the microtubule lattice but also with each other, once a first layer is bound to the microtubule surface (see Discussion). This apparent self-association phenomenon (i.e., MAP2c-MAP2c association) may well obscure an actual saturation of the rMAP2c binding sites on the microtubule surface. Because of the unusual stoichiometry, the data could not be fit to a simple microtubule-MAP binding model, and

Table 1[a]

[rMAP2c] (μM)	growth rate (μm/min)	shortening rate (μm/min)	fcat (cat/min gro)	fres (res/min sho)	#cat	#res	# mt	tgro (min)	tsho (min)	fr. sat. upper limit
0.0	2.36 ± 0.81	-44.0 ± 25.2	0.21 ± 0.03	0.82 ± 0.20	54	25	36	271.4	30.3	NA
0.038	2.28 ± 0.65	-42.5 ± 18.5	0.27 ± 0.08	0.85 ± 0.38	13	5	10	48.2	5.9	0.014
0.12	2.36 ± 0.65	-27.4 ± 18.6	0.24 ± 0.05	1.69 ± 0.39	19	18	13	80.3	11.2	0.028
0.17	2.85 ± 0.75	-33.5 ± 20.1	0.14 ± 0.06	2.02 ± 0.71	8	8	6	56.2	4.0	0.035
0.35	2.69 ± 0.79	-20.6 ± 7.5	0.06 ± 0.03	3.05 ± 1.4	5	5	12	83.4	1.6	0.055
0.53	2.96 ± 0.80	-21.8 ± 11.3	0.04 ± 0.03	2.34 ± 1.7	2	2	12	54.4	0.9	0.072
1.1	3.62 ± 1.0	no	no	no	no	no	22	74.0	no	0.14
3.7	3.71 ± 1.2	no	no	no	no	no	22	83.9	no	0.26

[a] no, no events observed; na, not applicable; fcat, frequency of catastrophe; fres, frequency of rescue; #cat, total number of observed catastrophes; #res, total number of observed rescues; #mt, total number of microtubules measured; tgro, total time of observed growth; tsho, total time of observed shortening; fr. sat. upper limit, estimated upper limit of the fractional saturation of rMAP2c binding (number of rMAP2c molecules bound per tubulin dimer).

equilibrium binding constants could not be determined. Nevertheless, it is clear from Figure 2 that rMAP2c binds to microtubules and that substantial levels of saturation (2 rMAP2c molecules bound per 100 tubulin dimers) of microtubules were reached at concentrations of rMAP2c in the range 0.02−0.1 μM. The binding curve of Figure 2 was employed to estimate the extent of saturation of the microtubule lattice at each of the concentrations of rMAP2c at which dynamic instability measurements were made (see Table 1).

To examine the effects that rMAP2c binding exerts on dynamics, this protein was added at concentrations in the 0−4 μM range to solutions of 10 μM tubulin. The microtubules formed under these conditions exhibited normal morphology when examined in video-enhanced DIC microscopy and by electron microscopy (Figure 3). Measurements of length vs time were carried out for a suitable number of individual microtubules at each concentration of rMAP2c. Some typical data obtained from plus ends (minus ends were not included in this study) are represented in Figure 4. From these data alone (compare Figure 4 panel A with panels B and C), it is apparent that rMAP2c has a dramatic stabilizing effect on the dynamic instability of microtubules. As the concentration of rMAP2c increased, the microtubules became less dynamic and spent more time in the growth phase. The surprising result, however, was the degree of stabilization of the microtubules. At relatively low concentrations of rMAP2c (1.1 μM rMAP2c to 10 μM tubulin) there is a complete suppression of dynamic instability, resulting in microtubules that exhibit only growth. Microtubules under these conditions grew out of the field of view very quickly, thereby reducing the amount of time a single microtubule could be observed. To compensate for the relatively short time during which a particular microtubule could be measured, a large number of microtubules were observed. Many short observations are equivalent to a smaller number of proportionately longer observations assuming all microtubules behave, on average, identically. Existing evidence (Gildersleeve et al., 1992) suggests that this is the case.

To quantitate the observations, an extensive series of length−time data were analyzed at each of the rMAP2c concentrations to obtain growth rate, shortening rate, frequency of catastrophe, and frequency of rescue. Results are summarized in Figures 5−7 and in Table 1. The most striking effect was the suppression of catastrophes at the higher observed concentrations of rMAP2c. As Figure 5A shows, the frequency of catastrophe decreased rapidly with increasing concentration of rMAP2c. When 1 μM rMAP2c

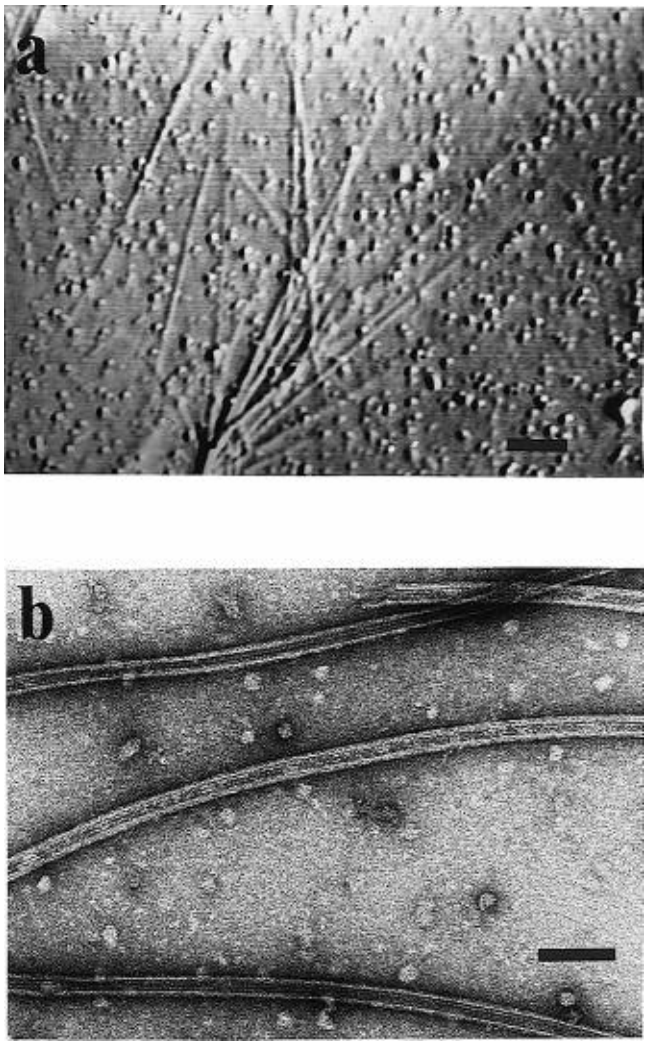

FIGURE 3: Microtubules grown in the presence of rMAP2c show normal morphology. (A) Video-enhanced DIC image of plus-ended microtubules nucleated from *Chlamydomonas* flagellar axonemal pieces in the presence of 3.7 μM rMAP2c and 10 μM tubulin. Scale bar = 2 μm. (B) Electron micrograph of plus-ended microtubules nucleated from *Chlamydomonas* flagellar axonemal pieces in the presence of 3.7 μM rMAP2c and 15 μM tubulin. Scale bar = 100 nm.

was reached, no catastrophes were detected in 74 min of observed growth and none were seen in 84 min at 3.7 μM rMAP2c. In contrast, control MAP-free microtubules underwent a catastrophe approximately every 5 min of observed growth (Table 1). In addition to catastrophes becoming less frequent, the mean length of a shortening excursion was seen

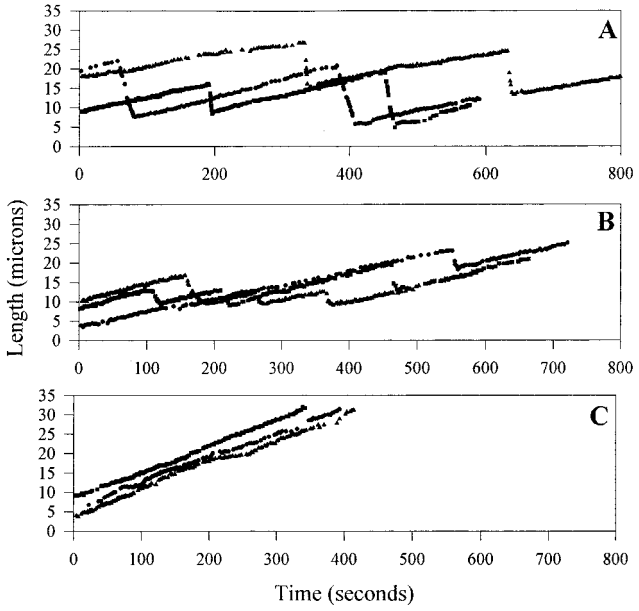

FIGURE 4: Typical measurements of lengths of individual microtubules over time, at constant concentration of tubulin and different concentrations of rMAP2c. Length−time data generated from measuring individual microtubules in real time at different concentrations of rMAP2c. (A) Control microtubules at 10 μM tubulin, with no rMAP2c added. (B) 10 μM tubulin with 0.12 μM rMAP2c added. (C) 10 μM tubulin with 3.7 μM rMAP2c added.

to decrease with increasing rMAP2c concentrations (Figure 5B). This diminution became apparent at 0.12 μM rMAP2c, a concentration at which the average length of a shortening excursion was roughly half that of control microtubules. The length of shortening excursions gradually became smaller with increasing rMAP2c concentrations until they fell below the level of detectability of light microscopy.

The mean growth rate of microtubules increased somewhat over the range of concentrations of rMAP2c tested (Figure 6 and Table 1). It remained apparently unchanged below a rMAP2c concentration of 0.17 μM, and increased 1.6-fold at the highest concentration tested (3.7 μM).

As the concentration of rMAP2c increased, the mean shortening rate of microtubules appeared to decrease gradually (Figure 7A). Measurement was rendered somewhat difficult in the concentration range above 0.17 μM because the reduced length and frequency of shortening excursions described in Figure 4 provided relatively few points to measure. These difficulties in measurement contributed to the large experimental uncertainty of these data and may also cause a systematic underestimation of the rates themselves. For instance, at 0.35 μM rMAP2c, only five shortening events were observed in about 85 min of growth (Table 1), and even fewer were observed at higher concentrations.

The frequency of rescue increased as the concentration of rMAP2c increased (Figure 7B). It is important to note that at high concentrations very few rescues were seen because very few catastrophes occurred. For example, at 0.53 μM rMAP2c, only two catastrophes were observed in 54 min of growth, providing a total of 0.85 min of shortening (Table 1). If the microtubules spend a small amount of their total time shortening, there can be very few transitions from shortening to growth. It is important to point out, though, that the few catastrophes that were seen at high concentrations of rMAP2c were quickly followed by rescues.

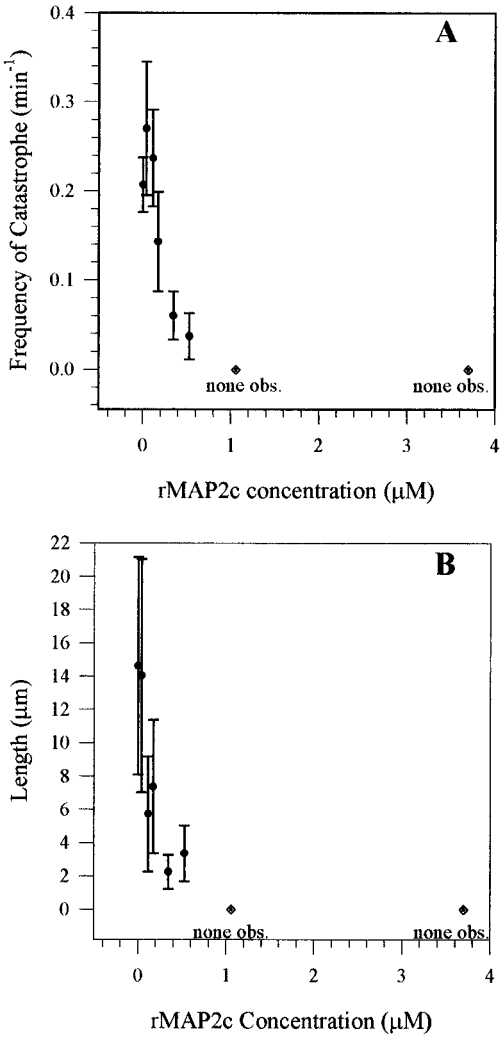

FIGURE 5: Frequency of catastrophe and average length of shortening excursions as functions of MAP2c concentration. (A) Frequency of catastrophe, determined at each rMAP2c concentration by dividing the total number of catastrophes by the total amount of time spent growing. Diamond-shaped points denote the fact that no catastrophes were observed at 1.1 μM rMAP2c in 74 min of growth or at 3.7 μM rMAP2c in 84 min of growth. Error bars represent 1 standard deviation. The standard deviation was estimated by dividing the square root of the number of events seen by the total time spent growing. (B) The average length of shortening events was determined for each rMAP2c concentration by dividing the total length of microtubule shortening events by the number of events observed. No shortening events were seen at 1.1 and 3.7 μM rMAP2c. Error bars represent 1 standard deviation.

Another interesting result seen with the addition of rMAP2c was the presence of apparent regions of stability on the microtubule. As Figure 8 shows, rescues appeared to occur at the same place on a microtubule on several occasions in the presence of low concentrations of rMAP2c (0.12 and 0.17 μM). This phenomenon was not observed in MAP-free controls. Once a rescue was observed at these concentrations and above, the microtubule did not shorten far beyond that point again. In the fifth example, lowest in the figure, the microtubule appears to have shortened approximately 1 μm beyond the previous rescue point during the subsequent two shortening events.

DISCUSSION

Protein Binding. From the binding isotherm in Figure 2 it is evident that recombinant MAP2c binds avidly to

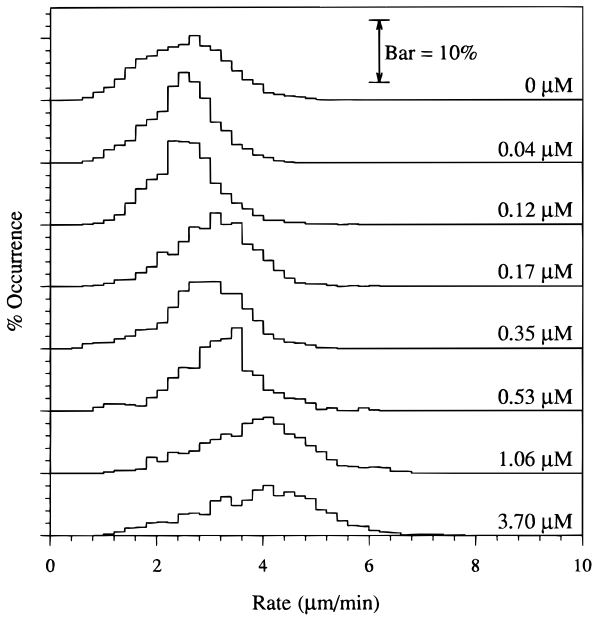

FIGURE 6: Microtubule growth rates as a function of MAP2c concentration. The graph depicts an outline of a histogram of the rate distribution at the specified concentrations of rMAP2c. Percent occurrence was determined by dividing the total number of rates per division by the total number of rates determined. Scale bar represents 10% occurrence.

microtubules. The amount that binds, however, is surprisingly large, exceeding one MAP bound per tubulin dimer and showing no sign of a plateau in the curve. Similar unusual behavior has been observed in other studies of MAP binding. Coffey and Purich (1995) studied binding of a construct consisting of the carboxyl terminus of bovine MAP2 (amino acids 1629 through 1828) in which repeat regions 1 and 3 were replaced with copies of region 2. Amounts bound reached 2.2 MAPs per tubulin dimer. In studies using native high molecular weight MAP2 purified biochemically, a lack of binding saturation is observed with tubulin/MAP2 ratios up to 1:1 (Wallis et al., 1993; compare their Figure 3 to the present Figure 2). Since MAP2c is of the same order of size as α- and β-tubulin, binding stoichiometries above one MAP2c per tubulin dimer would not be expected if a simple binding of MAP occurs on the outside of the tubulin lattice without extensive remodeling of the microtubule's structure (Jensen & Smaill, 1986; Hirokawa et al., 1988). Electron microscopic results (Figure 3) give no evidence of a major change in the microtubule's structure, so binding of more than one layer of MAPs must be invoked. Under buffer conditions similar to those used here, MAP2c was shown to form dimers in which the monomers are oriented antiparallel to each other as well as fibers up to 1.3 μm in length, the latter presumably involving parallel orientation of MAP2c monomers (Wille et al., 1992). Because no self-association of rMAP2c into sedimentable particles occurs in the absence of microtubules, and because oligomer formation in free solution does not occur at the concentrations employed in this study (Wille et al., 1992), we interpret the apparent high levels of binding as being due to self-association of the rMAP2c while it is bound to microtubules. The situation is represented schematically in Figure 9. Here, we intend only to suggest that the binding of a first layer of MAP2c, which must attach directly to the microtubular wall, facilitates in some way the binding of a

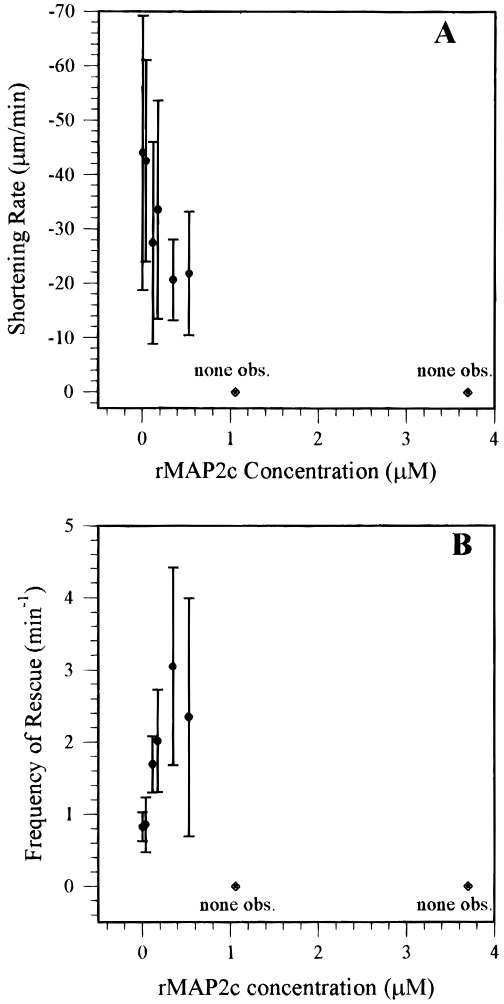

FIGURE 7: Microtubule shortening rates and frequencies of rescue as a function of rMAP2c concentration. (A) Shortening rates were measured in one-eighth speed slow motion playback. No shortening events were measured at 1.1 μM rMAP2c and 3.7 μM rMAP2c. Error bars represent 1 standard deviation. (B) Frequency of rescue was calculated by dividing the total number of rescues for a population of microtubules by the total time spent shortening for that population. No shortening events were seen at 1.1 μM rMAP2c and 3.7 μM rMAP2c, and therefore the frequency of rescue could not be calculated. Error bars represent 1 standard deviation. The standard deviation was calculated by dividing the square root of the number of events seen by the total time spent shortening. The small number of events observed due to the decreased amount of time spent shortening in the presence of higher concentrations of rMAP2c contribute to the increased size of error bars as the concentration of rMAP2c increases.

second, and perhaps further, layers of the protein, which must bind to MAP2c molecules already attached. The data do not permit one to determine, though, whether it is pre-existing oligomers of MAP2c that bind, or whether the binding of monomeric MAP2c molecules to the microtubule's wall facilitates, perhaps by a binding-dependent conformational change, the formation of MAP2c−MAP2c bonds. We have no direct evidence of the geometry, although the fiber-forming mode of association (Wille et al., 1992) could mediate the addition of several moles of rMAP2c per mole of tubulin dimer.

The likely formation by rMAP2c molecules of two kinds of bonds, those between the MAP and the microtubular wall and those between the MAP and other MAPs which in turn are bound to the wall, complicates detailed interpretation of the binding data by preventing the assignment of association

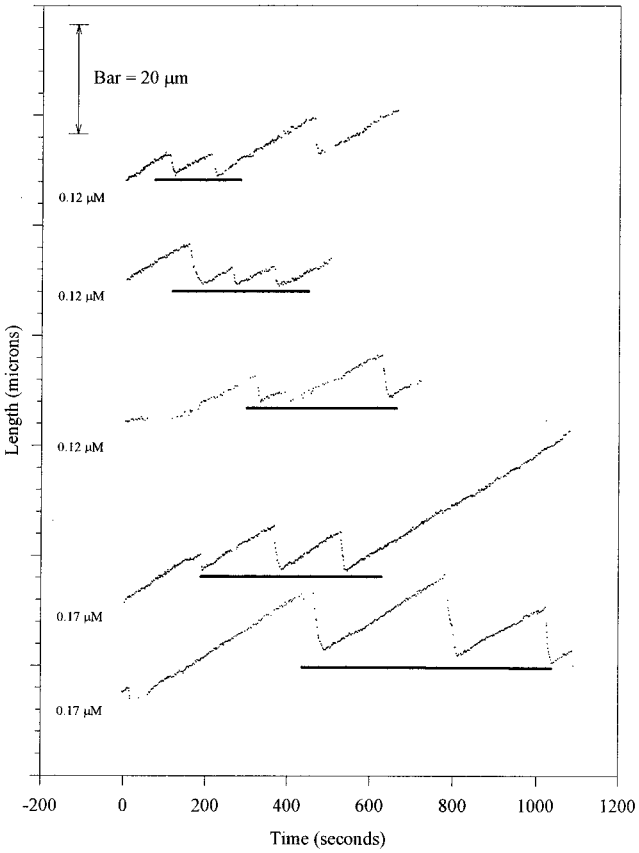

FIGURE 8: Apparent regions of stability on microtubules in the presence of rMAP2c. Five examples of regions of microtubules that were the site of two or more catastrophes at two different rMAP2c concentrations (0.12 and 0.17 μM). Once a catastrophe was seen at these concentrations or higher, the microtubule never shortened beyond that point again. The last example (lowest in this figure) shortened approximately 1 μm beyond the previous site of rescue in each of the subsequent two shortening events.

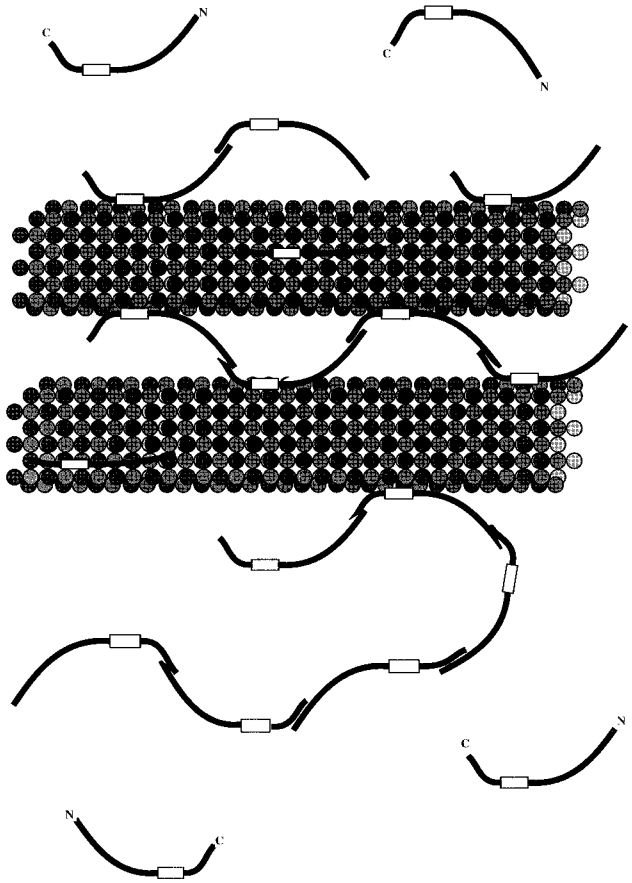

FIGURE 9: Model for microtubule-induced rMAP2c self-association. α- and β-subunits are represented as dark and light gray circles (the helicity of the tubulin lattice is not represented). rMAP2c molecules are represented by a a microtubule binding region (white box), a short carboxy-terminal region (short black line), and a long projection arm (long black line). The model depicts binding of rMAP2c to microtubules by the microtubule binding domain with no particular geometry. The carboxy-terminal ends and the projection arms are then free to associate with other rMAP2c molecules (either those bound to other microtubules or those free in solution). Tubulin dimers were modeled as having a repeat distance of 8 nm in the lattice. Microtubules were modeled as having a diameter of 28 nm. rMAP2c molecules were modeled as having a length of 48 nm (Wille et al., 1992). The spacing between microtubules is shown as 20 nm (Chen et al., 1992; Leclerc et al., 1996).

constants or cooperativity parameters with any certainty. Nevertheless, the region of the curve which encompasses the concentration range 0−1 μM, corresponding to the observations of dynamic instability, appears similar in shape to binding isotherms for other MAPs (Wallis et al., 1993; Gustke et al., 1994). The observed curve is useful because it allows one to determine the extent of binding of MAPs to microtubules, if not the actual fractional occupancy of sites on the microtubule lattice. It demonstrates that large changes in extent of binding accompany the changes in dynamic instability investigated here. Another implication of the presence of two types of binding is that the number of contacts between MAP2c and tubulin required to produce a particular level of suppression of dynamics must be even fewer than that estimated from the saturation.

Instability. MAPs have the general property of stabilizing microtubules *in vitro* (Pryer et al., 1992; Drechsel et al., 1992; Kowalski & Williams, 1993; Itoh & Hotani, 1994; Panda et al., 1995), and rMAP2c is no exception. As is the case with MAP2a/b and tau, rMAP2c exerts stabilizing effects on each of the four variables that characterize dynamic instability: it speeds growth, slows shortening, increases rescue frequency, and decreases catastrophe frequency. At a concentration between 0.53 and 1 μM, where 0.07 to 0.14 are the upper limits of MAPs bound per tubulin dimer, it suppresses catastrophes to such an extent that none could be detected in 74 min of observation.

At lower concentrations of rMAP2c, where some catastrophes occur, a strong stabilization is still seen. The approach to the catastrophe-free state can be appreciated from the concentration dependence of the mean length of a shortening event. As the concentration of rMAP2c increases, catastrophes become less frequent, and when they do occur they lead to much less shortening than do those in the MAP-free control. This diminution of shortening excursions is caused by the increase in frequency of rescue. From the shape of curves in Figure 5A,B, it appears that rMAP2c "squeezes out" shortening events by reducing their lengths until they are no longer detectable. Thus, even when the concentration of rMAP2c is low enough to allow catastrophes, its binding still tends to stabilize microtubules by modulating other variables.

Growth Rates and Frequency of Catastrophe. Microtubule growth rates in Figure 6 show the broad distribution characteristic of the dynamic instability process (Gildersleeve et al., 1992). rMAP2c shifts the distribution toward larger rates in a fashion qualitatively similar to that shown by

MAP2a/b (Kowalski & Williams, 1993), but with smaller apparent effects on its breadth. The decrease in catastrophe frequency accompanies this increase in growth rate.

Shortening Rates and Rescues. In common with MAP2a/b and tau (Drechsel et al., 1992; Kowalski & Williams, 1993), rMAP2c appears to decrease the rate at which microtubules depolymerize during shortening events (Figure 7A). Because MAP2c greatly reduces the lengths of shortening events, the uncertainties in measurement noted in Results make it difficult to determine the significance of this decrease in shortening rates. The slower shortening events are accompanied by a greater frequency of rescue when rMAP2c is added. This effect is most evident at the lower concentrations of rMAP2c, where many catastrophes still occur. At 0.12 μM rMAP2c, 18 rescues were seen in 11.22 min of shortening (Table 1). One would expect to see only nine rescues if the addition of rMAP2c had no effect on the microtubules. More dramatic increases in the rescue frequency are seen as the concentration of rMAP2c increases, although caution must be exercised in interpretation because the decreasing length of shortening events and the diminishing number of catastrophes makes the number of possible rescues very small.

Possible Differential Binding of MAP2c to the Cap and Body of Microtubules. The changes in growth rates and catastrophe frequency lag behind the changes in shortening rates and rescue frequency, in the sense that they become measurable only at substantially higher concentrations of MAP2c. Until the concentration reaches 0.17 μM, no measurable increase in growth rates or decrease in catastrophe frequency is seen (Table 1). At 0.17 μM, though, the mean shortening rate and rescue frequency are already substantially influenced. Changes in frequency of rescue occur at lower concentrations than do the changes in frequency of catastrophe. At 0.12 μM rMAP2c and 10 μM tubulin (a molar ratio of at least 90:1 tubulin/rMAP2c) the frequency of catastrophe was very similar to that of MAP-free microtubules. The frequency of rescue, however, was approximately double that of control microtubules (Table 1), causing the average length of the shortening events to be approximately half as long as those occurring in MAP-free microtubules (Figure 5B). Growth and catastrophe are events that occur at the *end* of a *growing* microtubule, and only those MAPs bound at the end are likely to influence them; shortening and rescue can also be influenced by MAPs bound to the wall of the body of the microtubule. The difference in effects seen at 0.17 μM might reflect a difference between the affinity of MAP2c for the wall and its affinity for the end or may represent differences in the effect exerted by a given density of bound MAPs.

Comparison with the Behavior of MAP2b and Tau: Binding. Differences in apparent modes of binding of MAPs (cooperativity, neighbor exclusion, etc.) preclude direct comparison of the affinity of MAP2c with that of other MAPs. In general, though, the binding data presented in this paper resemble those obtained by Wallis et al. (1993) with MAP2a/b over a comparatively narrow range of concentration (0−0.4 μM). The amounts of MAP bound at corresponding concentrations of free MAP as well as the shapes of the curves are similar in the two binding studies. The large extents of binding reported here were observed at concentrations of rMAP2c much higher than those employed with MAP2a/b, so it is not known whether similar results would be seen with that protein. Coffey and Purich (1995) reported binding studies of some MAP2 binding-domain constructs that lack the N-terminal projection arm. These molecules bound noncooperatively, with dissociation constants in the range 0.5−2 μM and a stoichiometry close to one MAP per tubulin dimer. Another construct, bearing three copies of the central repeat, exhibited a stoichiometry of 2.2 per tubulin dimer and displayed oligomerization in free solution, a result which accords with our supposition that MAP2c exhibits high levels of binding because of oligomerization. Various versions of tau, which do not form oligomers in solution (Gustke et al., 1994), bind noncooperatively with stoichiometry of approximately 0.5 per tubulin dimer and association constants in the micromolar range. We conclude that rMAP2c binds to microtubules in a manner that is influenced by oligomerization and with an affinity comparable to that of other known MAPs.

Dynamic Instability. rMAP2c, MAP2b, and tau all have similar stabilizing effects on the dynamic instability of microtubules, with subtle differences. Recombinant MAP2c has a *maximal* effect similar to that of recombinant tau (Drechsel et al., 1992), in that both completely suppress catastrophes at high concentrations. *In situ*, rMAP2c may have a stronger stabilizing effect on microtubules than tau, since at equimolar concentrations *in vitro* rMAP2c reduces catastrophes more strongly than does tau. Thus, at an approximate 30:1 molar ratio of tau to tubulin, tau decreased the catastrophe frequency of microtubules by a factor of 1.8 (Drechsel et al., 1992), whereas rMAP2c decreased the catastrophe frequency by a factor of 3.5 (Table 1).

Similarly, the stabilization produced by rMAP2c at equivalent molar concentration is greater than that produced by high molecular weight MAP2a/b (Kowalski & Williams, 1993), as judged by comparison of all four dynamic instability variables. The MAP2 used in the earlier study, however, was biochemically purified from brain and was undoubtedly a pool of many different posttranslationally modified forms of MAP2. This posttranslational modification, particularly phosphorylation (Jameson & Caplow, 1981; Murthy & Flavin, 1983; Burns et al., 1984; Hoshi et al., 1988; Brugg & Matus, 1991; Drechsel et al., 1992; Olesen, 1994; Ainsztein & Purich, 1994) may reduce its effectiveness as a modulator of dynamic instability, making comparison with unphosphorylated rMAP2c difficult.

Analyses of dynamic instability have followed the framework in Walker et al. (1988), which describes dynamic instability in terms of large (i.e., easily observable) excursions in length which are postulated to occur as unitary events. It is likely that, within one of these large growth events, a number of tiny (i.e., shorter than 500 subunits and thus not observable at light microscopic resolution) shortening events might be interpolated. If the binding of a rMAP2c reduced the frequency or size, or both, of such "microcatastrophes", the observable growth rate would seem to increase, even though the actual rate of tubulin association during assembly remained constant. This notion is supported by our observation that growth rates and frequency of catastrophe are both unchanged at lower rMAP2c concentrations, but when a decrease in the frequency of catastrophe is observed, there is a small, concomitant increase in the observed growth rate. It is possible that binding of rMAP2c to microtubules decreases the rate constant for dissociation of tubulin during the growth phase [k_{-1}^{e+} or k_{-1}^{e-}, in the notation of Walker

et al. (1988)], resulting in an increased net growth rate. In order to test this possibility, the value of k_{-1}^{e+} would have to be determined for microtubules in the presence of rMAP2c by varying the concentration of tubulin while keeping the concentration of rMAP2c constant. Such experiments were not performed for rMAP2c. Drechsel et al. (1992) performed such experiments with tau and discovered that the sum of k_{-1}^{e+} and k_{-1}^{e-} was essentially unaffected by tau. We cannot rule out the possibility that rMAP2c does, by some mechanism, enhance the actual rate of tubulin subunit addition, or retard the actual rate of subunit dissociation, independent of its effects on the frequencies of transitions.

Comparison to in Vivo Studies. Dhamodharan and Wadsworth (1995) studied the effects of microinjecting whole heat-stable brain MAPs and purified high molecular weight MAP2 into nonneuronal BSC-1 cells. Dynamic instability was suppressed *in vivo* in a fashion similar to the effects seen *in vitro* with rMAP2c. The frequency of catastrophe per unit time was reduced, and the frequency of rescue was increased. However, the growth rates of microtubules in MAP-injected cells also decreased, which led the authors to conclude that the concentration of tubulin, a variable held essentially constant in our experiments, is a limiting factor *in vivo*. The forms of heat-stable brain MAPs and MAP2 used in the *in vivo* work were purified from porcine brain and therefore most likely consisted of various phosphorylated forms, which might have been further altered after injection. These factors notwithstanding, it is clear that MAPs have similar stabilizing effects *in vivo* and *in vitro*.

CONCLUSIONS

The binding of fewer than one rMAP2c molecule per 10 tubulin dimers has a dramatic stabilizing effect on microtubules, exerted chiefly by stopping shortening events. Although the detailed geometry of binding is unknown, it is possible that, in a 13 protofilament microtubule, binding of a single molecule of MAP2c to a tubulin subunit within a given radial cross-section may be sufficient to arrest shortening at that point along the microtubule's length. Whether the block in shortening events results primarily from a decrease in catastrophe frequency or an increase in rescue frequency depends on the concentration of rMAP2c. At low concentrations, little or no change appears in the number of catastrophes, while there is a large effect on the rate of rescue and the length of catastrophe. Therefore, catastrophes may be stopped where rMAP2c is bound. However, at high concentrations, the growth rates of microtubules are increased and the frequency of catastrophe is decreased, indicating that rMAP2c is essentially stopping catastrophes at the growing end of the microtubule before they have a chance to begin. This biochemical property could be extremely important in creating long stabilized microtubules during dendritic elongation and arborization, events which correlate with high expression levels of MAP2c.

The recombinant MAP2c employed in this study is free of posttranslational modifications. Since it has been shown that MAP activity can be altered by the sites and amount of phosphorylation (Jameson & Caplow, 1981; Murthy & Flavin, 1983; Burns et al., 1984; Hoshi et al., 1988; Brugg & Matus, 1991; Drechsel et al., 1992; Olesen, 1994; Ainsztein & Purich 1994), and since MAP2c is phosphorylated *in vivo* (Crandall & Fischer, 1989), it will be important in the future to determine the way in which phosphorylation modulates the stabilizing effect of rMAP2c. The present study can be regarded as a first step in that effort. If the effects of phosphorylation on the stabilizing nature of rMAP2c can be determined and then correlated to the phosphorylation state of MAP2c during neuronal development, we will move closer to understanding how a cell controls microtubule dynamics in order to create specialized cytoskeletons.

ACKNOWLEDGMENT

We thank Dr. Paula Flicker and Ms. Melissa Peterson for expert electron microscopy and Ms. Sandra Won for help in the preparation of rMAP2c. The programs for measurement and analysis of microtubule growth and shortening were written by Dr. Martin Billger and revised by Mr. Eric Hagstrom. We also thank Ms. Audrey Lamb and Dr. Susan Pedigo for critical reading of the manuscript.

REFERENCES

Ainsztein, A. M., & Purich, D. L. (1994) *J. Biol. Chem. 269*, 28465−28471.
Baas, P. W., Pienkowski, T. P., & Kosik, K. S. (1991) *J. Cell Biol. 115*, 1333−1344.
Berling, B., Wille, H., Roll, B., Mandelkow, E. M., Garner, C., & Mandelkow, E. (1994) *Eur. J. Cell Biol. 64*, 120−130.
Bradford, M. M. (1976) *Anal. Biochem. 72*, 248−254.
Bré, M. H., & Karsenti, E. (1990) *Cell Motil. Cytoskeleton 15*, 88−98.
Brugg, B., & Matus, A. (1991) *J. Cell Biol. 114*, 735−743.
Burns, R. G., Islam, K., & Chapman, R. (1984) *Eur. J. Biochem. 141*, 609−615.
Cassimeris, L. (1993) *Cell Motil. Cytoskeleton 2*, 275−281.
Cassimeris, L. U., Pryer, N. K., & Salmon, E. D. (1988) *J. Cell Biol. 107*, 2223−2231.
Charriere-Bertrand, C., Garner, C., Tardy, M., & Nunez, J. (1991) *J. Neurochem. 56*, 385−391.
Chen, J., Kanai, Y., Cowan, N. J., & Hirokawa, N. (1992) *Nature 360*, 674−677.
Chung, W. J., Kindler, S., Seidenbecher, C., & Garner, C. C. (1996) *J. Neurochem. 66*, 1273−1281.
Cleveland, D. W., Hwo, S.-Y., & Kirschner, M. W. (1977) *J. Mol. Biol. 116*, 207−225.
Coffey, R. L., & Purich, D. L. (1995) *J. Biol. Chem. 270*, 1035−1040.
Correia, J. J., Baty, L. T., & Williams, R. C., Jr. (1987) *J. Biol. Chem. 262*, 17278−17284.
Crandall, J. E., & Fischer, I. (1989) *J. Neurochem. 53*, 1910−1917.
Dhamodharan, R., & Wadsworth, P. (1995) *J. Cell Sci. 108*, 1679−1689.
Drechsel, D. N., Hyman, A. A., Cobb, M. H., & Kirschner, M. W. (1992) *Mol. Biol. Cell 3*, 1141−1154.
Gallo, Jean-M., Hanger, D. P., Twist, E. C., Kosik, K. S., & Anderton, B. H. (1992) *Biochem. J. 286*, 399−404.
Gamblin, T. C., & Williams, R. C., Jr. (1995) *Anal. Biochem. 232*, 43−46.
Garner, C. C., & Matus, A. (1988) *J. Cell Biol. 106*, 779−783.
Gildersleeve, R. F., Cross, A. R., Cullen, K. E., Fagen, A. P., & Williams, R. C., Jr. (1992) *J. Biol. Chem. 267*, 7995−8006.
Gustke, N., Trinczek, B., Biernat, J., Mandelkow, E.-M., & Mandelkow, E. (1994) *Biochemistry 33*, 9511−9522.
Hirokawa, N., Shiomura, Y., & Okabe, S. (1988) *J. Cell Biol. 107*, 1449−1459.
Horio, T., & Hotani, H. (1986) *Nature 321*, 605−607.
Hoshi, M., Akiyama, T., Shinohara, Y., Miyata, Y., Ogawara, H., Nishida, E., & Sakai, H. (1988) *Eur. J. Biochem. 174*, 225−230.
Hush, J. M., Wasdsorth, P., Callaham, D. A., & Hepler, P. K. (1994) *J. Cell Sci. 107*, 775−784.
Itoh, T. J., & Hotani, H. (1994) *Cell Struct. Funct. 19*, 279−290.

Jameson, L., & Caplow, M. (1981) *Proc. Natl. Acad. Sci. U.S.A. 78*, 3413−3417.
Jensen, C. G., & Smaill, B. H. (1986) *J. Cell Biol. 103*, 559−569.
Job, D., Pabion, M., & Margolis, R. L. (1985) *J. Cell Biol. 101*, 1680−1689.
Kanai, Y., Takemura, R., Oshima, T., Mori, H., Ihara, Y., Yanagisawa, M., Masaki, T., & Hirokawa, N. (1989) *J. Cell Biol. 109*, 1173−1184.
Kindler, S., Schulz, B., Goedert, M., & Garner, C. C. (1990) *J. Biol. Chem. 265*, 19679−19684.
Knops, J., Kosik, K. S., Lee, G., Pardee, J. D., Cohen-Gould, L., & McConlogue, L. (1991) *J. Cell Biol. 114*, 725−733.
Knowles, R., LeClerc, N., & Kosik, K. S. (1994) *Cell Motil. Cytoskeleton 28*, 256−264.
Kowalski, R. J., & Williams, R. C., Jr. (1993) *J. Biol. Chem. 268*, 9847−9855.
Leclerc, N., Kosik, K. S., Cowan, N., Pienkowski, T. P., & Baas, P. W. (1993) *Proc. Natl. Acad. Sci. U.S.A. 90*, 6223−6227.
Leclerc, N., Baas, P. W., Garner, C. C., & Kosik, K. S. (1996) *Mol. Biol. Cell 7*, 443−455.
Lewis, S. A., Ivanov, I. E., Lee, G. H., & Cowan, N. J. (1989) *Nature 342*, 498−505.
Markwell, M. A. K. (1982) *Anal. Biochem. 125*, 427−432.
Mitchison, T., & Kirschner, M. W. (1984a) *Nature 312*, 237−242.
Mitchison, T., & Kirschner, M. W. (1984b) *Nature 312*, 232−237.
Murphy, D. B., & Borisy, G. G. (1975) *Proc. Natl. Acad. Sci. U.S.A. 72*, 2696−2700.
Murphy, D. B., Johnson, K. A., & Borisy, G. G. (1977) *J. Mol. Biol. 117*, 33−52.
Murthy, N., & Flavin, M. (1983) *Eur. J. Biochem. 137*, 37−46.
Okabe, S., & Hirokawa, N. (1988) *J. Cell Biol. 107*, 651−664.
Olesen, O. F. (1994) *J. Biol. Chem. 269*, 32904−32908.
Olson, K. R., McIntosh, J. R., & Olmsted, J. B. (1995) *J. Cell Biol. 130*, 639−650.
Panda, D., Goode, B. L., Feinstein, S. C., & Wilson, L. (1995) *Biochemistry 34*, 11117−11127.
Pryer, N. K., Walker, R. A., Skeen, V. P., Bourns, B. D., Soboeiro, M. F., & Salmon, E. D. (1992) *J. Cell Sci. 103*, 965−976.
Riederer, B. M. (1992) *Histochem. J. 24*, 783−790.
Riederer, B. M., & Matus, A. (1985) *Proc. Natl. Acad. Sci. U.S.A. 82*, 6006−6009.
Sammak, P. J., & Borisy, G. G. (1988) *Nature 332*, 724−726.
Sanchez, C., Diaz-Nido, J., & Avila, J. (1995) *Biochem. J. 306*, 481−487.
Schnapp, B. J. (1986) *Methods Enzymol. 134*, 561−574.
Schulze, E., & Kirschner, M. W. (1988) *Nature (News and Views) 334*, 356−359.
Shelden, E., & Wadsworth, P. (1993) *J. Cell Biol. 120*, 935−945.
Sloboda, R. D., Dentler, W. L., & Rosenbaum, J. L. (1976) *Biochemistry 15*, 4497−4505.
Takemura, R., Okabe, S., Umeyama, T., Kanai, Y., Cowan, N. J., & Hirokawa, N. (1992) *J. Cell Sci. 103*, 953−964.
Takemura, R., Okabe, S., Umeyama, T., & Hirokawa, N. (1995) *Mol. Biol. Cell 6*, 981−996.
Tucker, R. P. (1990) *Brain Res. Rev. 15*, 101−120.
Umeyama, T., Okabe, S., Kanai, Y., & Hirokawa, N. (1993) *J. Cell Biol. 120*, 451−465.
Vallee, R. B. (1982) *J. Cell Biol. 92*, 435−442.
Vallee, R. B. (1986) *Methods Enzymol. 134*, 89−104.
Vasquez, R. J., Gard, D. L., & Cassimeris, L. (1994) *J. Cell Biol. 127*, 985−993.
Walker, R. A., O'Brien, E. T., Pryer, N. K., Soboeiro, M. F., Voter, W. A., Erickson, H. P., & Salmon, E. D. (1988) *J. Cell Biol. 107*, 1437−1448.
Wallis, K. T., Azhar, S., Rho, M. B., Lewis, S. A., Cowan, N. J., & Murphy, D. B. (1993) *J. Biol. Chem. 268*, 15158−15167.
Weisshaar, B., & Matus, A. (1993) *J. Neurocytol. 22*, 727−734.
Weisshaar, B., Doll, T., & Matus, A. (1992) *Development 116*, 1151−1161.
Wille, H., Mandelkow, E. M., & Mandelkow, E. (1992) *J. Biol. Chem. 267*, 10737−10742.
Williams, R. C., Jr. (1992) in *The Cytoskeleton, A Practical Approach*, pp 151−166, Oxford University Press, Oxford.
Williams, R. C., Jr., & Lee, J. C. (1982) *Methods Enzymol. 85*, 376−385.
Witman, G. B. (1986) *Methods Enzymol. 134*, 280−290.
Yamauchi, P. S., Flynn, G. C., Marsh, R. L., & Purich, D. L. (1993) *J. Neurochem. 60*, 817−826.

BI961135D